ROI SELECTION IN MICROCALCIFICATION DETECTION

László LASZTOVICZA
Advisor: Béla PATAKI

I. Introduction

Microcalcifications are small bright spots and they are usually grouped into clusters in mammographic images. An image can contain more than one cluster but still the area of the clusters is far smaller than the area of the breast. The aim of ROI (region of interest) selection is to select suspicious areas which can contain microcalcifications for further analysis. A proper ROI selection method can increase the overall processing speed and more importantly it can decrease the number of false positive detections. Microcalcification detection algorithms use different strategies to select ROIs. In [1] a wavelet and fuzzy c-means based method is presented. A wavelet based method using an adaptive homomorphic enhancement filter can be found in [2], other classical filter based method in [3] or morphological filtering in [4]. Another strategy can be subtracting the background and using a threshold to detect suspicious pixels and regions [5]. A relevance vector machine based approach is used in [6] and a method applying ant colony optimization and genetic algorithms is presented in [7]. Texture based methods are also exist [8, 9] with rather good performance.

In the present paper we discuss a method for ROI selection and give some modifications in order to improve its performance.

II. Surrounding region dependence method

A. Surrounding region dependence matrix

Surrounding region dependence method (SRDM) is a texture based method for detecting ROIs [8, 9]. For every image pixel (x, y) in the image plane $L_x \times L_y$ we define three windows which give us two regions R_1 and R_2 (see Figure 1). Then we define a matrix using a threshold q,

$$M(q) = \lfloor \alpha_{ij} \rfloor, \quad 0 \le i \le m, \quad 0 \le j \le n, \qquad (1)$$

where m and n are the number of pixels in regions R_1 and R_2 and

$$\alpha_{ij} = \#\{(x, y) \mid c_{R_1}(x, y) = i \wedge c_{R_2}(x, y) = j; (x, y) \in L_x \times L_y\}. \qquad (2)$$

The counters c_{R_1} and c_{R_2} define the number of those pixels in the surrounding regions R_1 and R_2 where the difference in the intensity is greater compared to the central pixel and defined as,

$$c_{R_1}(x, y) = \#\{(k,l) \mid (k,l) \in R_1 \wedge [S(x, y) - S(k,l)] > q\} \qquad (3)$$

$$c_{R_2}(x, y) = \#\{(k,l) \mid (k,l) \in R_2 \wedge [S(x, y) - S(k,l)] > q\} \qquad (4)$$

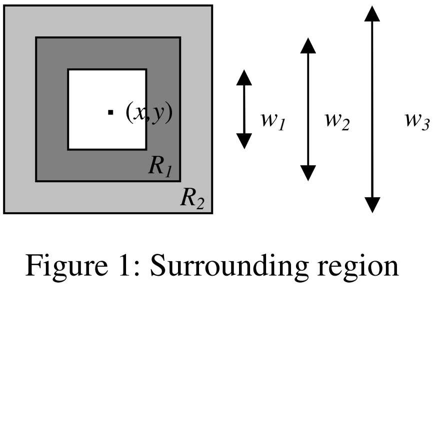

Figure 1: Surrounding region

The α_{ij} elements of the matrix $M(q)$ are the number of those pixels in the image whose difference in the intensity value compared to the pixels in the surrounding regions is greater than the threshold q.

B. Feature selection

Let N is the sum of the elements of the matrix $M(q)$, and $r(i, j)$ is the reciprocal of the elements,

$$N = \sum_{i=0}^{m}\sum_{j=0}^{n}\alpha(i, j);\ r(i, j) = \begin{cases} \dfrac{1}{\alpha(i, j)}, & \text{if } \alpha(i, j) > 0, \\ 0, & \text{otherwise.} \end{cases}$$

Then following [8, 9] the features shown in Table 1 can be extracted from the matrix $M(q)$.

Table 1: Features to be extracted from $M(q)$

Horizontal Weighted Sum	Vertical Weighted Sum
$HWS = \frac{1}{N}\sum_{i=0}^{m}\sum_{j=0}^{n} i^2 r(i, j)$	$VWS = \frac{1}{N}\sum_{i=0}^{m}\sum_{j=0}^{n} j^2 r(i, j)$
Diagonal Weighted Sum	Grid Weighted Sum
$DWS = \frac{1}{N}\sum_{k=0}^{m+n} k^2 \left(\sum_{\substack{i=0 \\ i+j=k}}^{m} \sum_{j=0}^{n} r(i, j) \right)$	$GWS = \frac{1}{N}\sum_{i=0}^{m}\sum_{j=0}^{n} ijr(i, j)$

For each ROI a matrix is computed then the four features are extracted. The feature vectors serve as input to a neural network which performs the classification of the ROI either as negative or positive.

III. Improving the SRMD method

Though the method itself provides fairly good results I introduced some modifications to further improve the performance.

A. Image enhancement and feature extraction

First I introduced an image enhancement step. The enhanced image was then used as input to the SRDM method instead of the original image. The enhanced image can also be considered as a feature image and can be used in the detection of microcalcification clusters provided the ROI was evaluated as positive. The image enhancement is as follows. The input ROI is first filtered with an averaging filter then the filtered ROI is subtracted from the original one. For every pixel the following neighborhood operation is carried out

$$S_{diff}(x, y) = S(x, y) - \frac{1}{n}\sum_{i, j \in W} S(i, j), \quad (5)$$

where W is a fixed sized window or kernel with size n centered around (x, y) with intensity $S(x, y)$.

From some pilot measurement the kernel size was determined in 21 pixels, however for some settings other kernels also had a similar performance. Therefore I introduced a simple modification. As the brightest pixels are around the center of the microcalcifications at least locally, it is likely that the average will decrease as the kernel size is increasing. For every pixel a series of average values can be determined using different kernel size (e.g. 13, 15, 17 … pixels) according to the size of the individual microcalcifications. Then for every pixel I chose the feature value given by Eq. (5) where the average reached minimum.

B. Introducing new features

In order to further enhance the performance of ROI selection I introduced three more features that are not related to the SRDM matrix. The features are extracted from the ROI after the enhancement step. For each ROI two sums were computed. First summing the intensity values by rows and second summing them by columns. That gives us two vectors (e.g. vertical and horizontal sums): $F_1(r) = \sum_c S(r,c)$ and $F_2(c) = \sum_r S(r,c)$. Then two features are simply the standard deviation of the vertical and horizontal sums F_1 and F_2. The third feature was simply the standard deviation of the intensity values in the input image. Analyzing the new features they show good characteristics in discriminating capability.

IV. Experiments and results

For the experiments 200 positive and 200 negative ROIs were extracted from images of the DDSM database [10]. In the experiments I used a 10-fold cross-validation setting in order to determine the optimal setting of the parameters for the method and to measure the performance of the algorithm and the proposed improvements. Neural networks were used as classifiers. The neural networks had one hidden layer with 8 neurons and with tangent hyperbolic nonlinearity. The number of inputs was determined by the number of features. For the SRMD method the number of input features is 4 while for the extended method it is 7.

The parameters of the SRDM method are the size of the windows (w_1, w_2, w_3) and the threshold q. For the proposed improvements the effect of the new features (*input – std* stands for the new features) and the size of the kernel (w_4 – *avg* stands for the procedure for choosing feature value presented in section III) for the feature extraction/image enhancement step. I also examined the case when the samples in the training set containing microcalcifications are doubled to increase the error if a sample containing microcalcification is misclassified (*tr_set*) and the case when the resolution of the image is decreased (*res* - size of an input ROI in pixels). The classification accuracy for the cross-validation is also presented (*acc*). Table 2 shows the 4 best results and the best result for the original method (in light gray). The meaning of the columns is explained above. In Table 2 the results are given as the area under the ROC curve (A_z) and the 95% confidence interval for the A_z value is also given

Table 2: The best results for different parameter settings

w_1	w_2	w_3	q	w_4	res	tr_set	input	A_z	confidence (95%)
3	7	11	11	21	256x256	-	SRDM + std	0.959	0.921 to 0.982
5	7	9	8	avg	256x256	-	SRDM	0.958	0.920 to 0.981
3	7	11	8	avg	256x256	-	SRDM	0.957	0.918 to 0.980
3	5	7	7	21	128x128	-	SRDM + std	0.954	0.915 to 0.979
3	7	11	11	-	256x256	-	SRDM	0.949	0.909 to 0.975

. The ROC curves for the best result reached by the original and the modified method are shown in Figure 2.

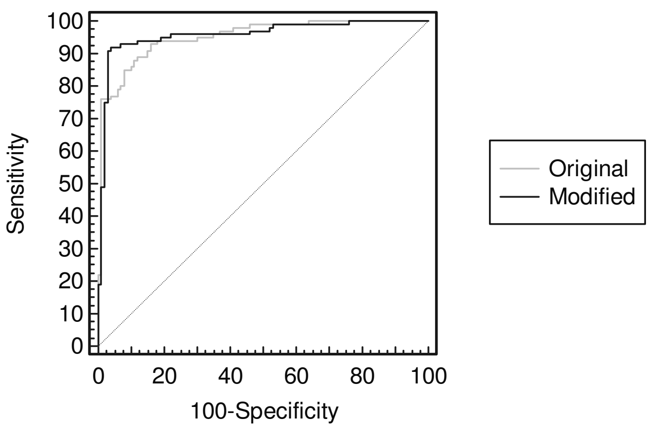

Figure 2: ROC curves for the best results

As it can be seen from Table 2 the results are very similar and there is no statistically significant difference in the results. Still they show that by using the introduced new features and using enhanced images as inputs the performance can be increased. It is also interesting that fairly good result can be reached even when the resolution of the input ROI is halved which can make the processing faster. The best results were reached by the improved method which proves its viability.

In Figure 2 though there are no significant differences between the ROC curves it can be seen that the modified method reached higher sensitivity at higher specificity therefore it improved the original methods by decreasing false positive detections.

V. Conclusion and discussion

The proposed modifications to the original SRDM method were using enhanced or feature images as input images and introducing new features which expresses the variability of pixel values in rows, columns and in the image itself. As it can be seen from the results the modified method is capable of reaching better performance than the original one. Future experiments are required to prove that on larger datasets. It is also true however, that there is no statistically significant difference between the best results at this point, therefore either the number of samples is too low to reach any significant conclusion or there is no real difference between the methods and the selection of parameters. The latter suggests using combined classifiers as the difference between the different parameter settings is not significant – they are giving good results in themselves – but they are mistaken in possibly different cases. Another way can be to find adaptive selection algorithms for the different parameters. Finally the two ways can be combined into a hierarchical multiple classifier system.

References

[1] S. Sentelle, C. Sentelle, and M. A. Sutton, "Multiresolution-based segmentation of calcifications for the early detection of breast cancer," *Real-Time Imaging*, vol. 8, no. 3, pp. 237–252, 2002.

[2] H.-K. Kang, S.-M. Kim, N. N. Thanh, Y. M. Ro, and W.-H. Kim, "Adaptive microcalcification detection in computer aided diagnosis," in *Computational Science - ICCS 2004, 4th International Conference, Kraków, Poland, June 6-9, 2004, Proceedings, Part IV*, ser. Lecture Notes in Computer Science, M. Bubak, G. Albada, P. Sloot, and J. Dongarra, Eds., vol. 3039. Springer-Verlag Berlin Heidelberg, 2004, pp. 1110–1117.

[3] P. Pettazzoni, G. Pallotti, M. Mattina, and C. Leoni, "Computerized detection of clustered microcalcifications: a modular approach with non-linear filters," *Medical Hypotheses*, vol. 56, no. 4, pp. 442–447, 2001.

[4] J. C. Yang, J. W. Shin, G. S. Yang, and D. S. Park, "Microcalcifications detection in digital mammogram using morphological bandpass filters," in *Computational and Information Science, First International Symposium, CIS 2004, Shanghai, China, December 16-18, 2004. Proceedings*, ser. Lecture Notes in Computer Science, J. Zhang, J.-H. He, and Y. Fu, Eds., vol. 3314. Springer-Verlag Berlin Heidelberg, 2004, pp. 492–497.

[5] A. Papadopoulos, D. I. Fotiadis, and A. Likas, "An automatic microcalcification detection system based on a hybrid neural network classifier," *Artificial Intelligence in Medicine*, vol. 25, no. 2, pp. 149–167, 2002.

[6] W. Liyang, Y. Yongyi, R. M. Nishikawa, M. N. Wernick, and A. Edwards, "Relevance vector machine for automatic detection of clustered microcalcifications," *Medical Imaging, IEEE Transactions on*, vol. 24, no. 10, pp. 1278–1285, 2005.

[7] K.Thangavel, M.Karnan, R.Sivakumar, and A. K. Mohideen, "Ant colony system for segmentation and classification of microcalcification in mammograms," *The International Journal of Artificial Intelligence and Machine Learning*, vol. 5, 2005.

[8] J. K. Kim and H. W. Park, "Statistical textural features for detection of microcalcifications in digitized mammograms," *Medical Imaging, IEEE Transactions on*, vol. 18, no. 3, pp. 231–238, 1999.

[9] J. K. Kim, J. M. Park, K. S. Song, and H. W. Park, "Detection of clustered microcalcifications on mammograms using surrounding region dependence method and artificial neural network," *The Journal of VLSI Signal Processing*, vol. 18, no. 3, pp. 251–262, Apr. 1998.

[10] M. Heath, K. Bowyer, D. Kopans, R. Moore, and W. P. Kegelmeyer, "The digital database for screening mammography," in *Proceedings of the Fifth International Workshop on Digital Mammography*, M. Yaffe, Ed. Medical Physics Publishing, 2001, pp. 212–218.